Check for updates

WO₃/BiVO₄ photoanode coated with mesoporous Al₂O₃ layer for oxidative production of hydrogen peroxide from water with high selectivity†

Kojiro Fuku, [ID] *[a] Yuta Miyase,[ab] Yugo Miseki, [ID] [a] Takahiro Gunji[ab] and Kazuhiro Sayama*[ab]

A WO₃/BiVO₄ photoanode coated with various metal oxides demonstrated high selectivity (faradaic efficiency) for hydrogen peroxide (H_2O_2) generation from water (H_2O) under irradiation of simulated solar light in a highly concentrated hydrogen carbonate ($KHCO_3$) aqueous solution. A mesoporous and amorphous aluminium oxide (Al_2O_3) layer significantly facilitated inhibition of the oxidative degradation of generated H_2O_2 into oxygen (O_2) on the photoanode, resulting in unprecedented H_2O_2 selectivity (ca. 80%) and the accumulation (>2500 μM at 50C).

Chemical conversions using light energy have been performed in various fields since the discovery of the Honda–Fujishima effect.[1–25] Significant efforts have recently been devoted to H_2 production by water splitting using inexhaustible light for clean energy conversion processes.[1–4,8–29] Photoelectrode systems are widely recognised as a promising technology for H_2 production because they operate at an electrolysis voltage lower than the theoretical electrolysis voltage of water (<1.23 V).[1,8–29] Visible light-responsive oxide photoanodes with a narrow bandgap energy, such as WO₃, BiVO₄ and Fe₂O₃, are desirable for the efficient utilisation of solar light and economical synthetic processes.[8–29] Most importantly, numerous efforts have been focused on BiVO₄ photoanodes capable of utilising a wide range of light energy (∼520 nm) and achieving efficient O₂ generation by water splitting.[9–21,28,29,32] A WO₃/BiVO₄ photoanode that combines BiVO₄ with a WO₃ underlayer for the efficient transfer of excited electrons on BiVO₄ to the F-doped SnO₂ conductive glass (FTO) substrate shows exceptional photoelectrochemical performance for water splitting into H₂ and O₂.[10–13,17–20,28,29,32] However, most previous investigations, containing electrochemical reactions, focused solely on the recovery of H₂ energy generated on the cathode and little attention was paid to the recovery of the oxidation products simultaneously evolved during water splitting.[24–31]
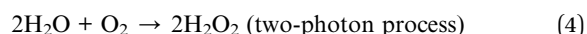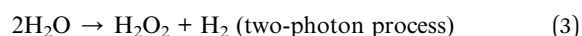
[a]Research Center for Photovoltaics (RCPV), National Institute of Advanced Industrial Science and Technology (AIST), Central 5, 1-1-1 Higashi, Tsukuba, Ibaraki 305-8565, Japan. E-mail: k.sayama@aist.go.jp

[b]Department of Pure and Applied Chemistry, Tokyo University of Science, 2641 Yamasaki, Noda, Chiba 278-8514, Japan

H_2O_2 is an especially versatile and clean oxidation product having the potential to generate instead of O_2 from H_2O (eqn (1)).

$$2H_2O \rightarrow H_2O_2 + 2H^+ + 2e^- \quad (E(H_2O_2/H_2O) = +1.77 \text{ V } vs. \text{ RHE}) \tag{1}$$
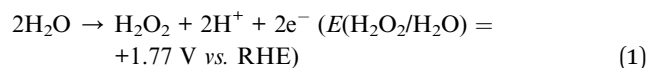
However, the accumulation of H_2O_2, generated oxidatively is extremely difficult because degradation of H_2O_2 into O_2 also occurs easily and oxidatively in a conventional photo-electrochemical system i.e. the redox potential of H_2O_2 degradation is more negative than the redox potential of H_2O_2 production from H_2O (eqn (1) and (2)), resulting in low selectivity for oxidative H_2O_2 generation.

$$H_2O_2 \rightarrow O_2 + 2H^+ + 2e^- \quad (E(O_2/H_2O_2) = +0.68 \text{ V } vs. \text{ RHE}) \tag{2}$$
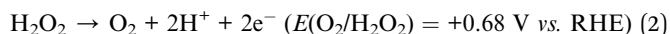
Recently, we reported that a photoelectrochemical system combining the WO₃/BiVO₄ photoanode and aqueous electrolyte of KHCO₃ under CO₂ bubbling could achieve simultaneous generation and accumulation of H_2O_2 and H_2 from H_2O (eqn (3)).[28,29] In this system, the aqueous electrolyte of KHCO₃ acts as an excellent oxidative catalyst for generating H_2O_2 from H_2O. Moreover, H_2O_2 could be produced at no external bias on both a WO₃/BiVO₄ photoanode (from H_2O) and an Au cathode (from O_2) via a two-photon process (eqn (4)).[29]

$$2H_2O \rightarrow H_2O_2 + H_2 \quad \text{(two-photon process)} \tag{3}$$

$$2H_2O + O_2 \rightarrow 2H_2O_2 \quad \text{(two-photon process)} \tag{4}$$

Although the selectivity (faradaic efficiency: $\eta(H_2O_2)$) of reductive H_2O_2 production from O_2 on cathodes such as Au was very high, almost 100%, the maximum selectivity ($\eta(H_2O_2)$) for oxidative H_2O_2 production on WO₃/BiVO₄ photoanodes was still

low, only *ca.* 54%. The design of novel photoanodes capable of achieving efficient H_2O_2 generation and inhibiting oxidative degradation of generated H_2O_2 is absolutely imperative for building a clean and breakthrough technology, by accumulating H_2O_2 and H_2 with unprecedented H_2O_2 selectivity using only H_2O as the raw material.

Here, we focused on a surface modification of the metal oxide (MeO_x) layers on the $WO_3/BiVO_4$ photoanode surface to achieve excellent selectivity of generation and accumulation of H_2O_2 in the $KHCO_3$ aqueous solution under simulated solar light irradiation (Fig. 1). The MeO_x layers were prepared by spin-coating of metal organic solutions and calcination. Introducing a porous Al_2O_3 layer was found to specifically permit oxidative H_2O_2 generation and accumulation with exceptional selectivity in an aqueous $KHCO_3$ electrolyte because of the blocking effect of oxidative degradation of the generated H_2O_2 into O_2 on the photoanode.

Details regarding experimental procedures for preparation and photoelectrochemical reactions of photoanodes are provided in the ESI†.

The effects of MeO_x layers, modified on the $WO_3/BiVO_4$ photoanode, for oxidative H_2O_2 generation properties were investigated at an applied electric charge of 0.9C (900 s at steady photocurrent of 1 mA) in a 0.5 M $KHCO_3$ aqueous electrolyte. As shown in Fig. 2, all MeO_x-coated photoanodes, except CoO_x, enhanced the oxidative H_2O_2 generation compared to a bare $WO_3/BiVO_4$ photoanode, and the enhanced effect, ranked by the modified metal oxide, was $Al_2O_3 > ZrO_2 > TiO_2 > SiO_2 \gg CoO_x$. Little H_2O_2 was observed on the CoO_x coated photoanode, because CoO_x probably decomposed the generated H_2O_2 quickly, or O_2 may be evolved on CoO_x directly. It should be noted that the Al_2O_3 modification on the $WO_3/BiVO_4$ photo-anode achieved roughly twice the oxidative H_2O_2 generation compared to the bare $WO_3/BiVO_4$ photoanode. The Al_2O_3 uniformly, smoothly and flatly covered the entire area of the $WO_3/BiVO_4$ photoanode as shown in the SEM images (Fig. 3), whereas other MeO_x were granularly and uniformly supported on that and possessed any crack holes (Fig. S1; ESI†). It was also confirmed, from XRD measurement (Fig. S2; ESI†), that no
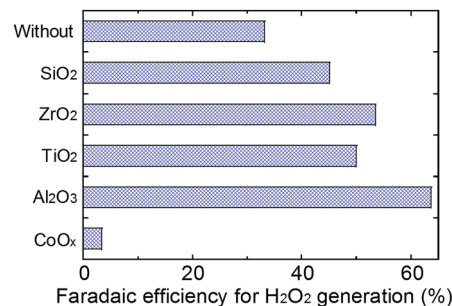

Fig. 2 Oxidative H_2O_2 generation on photoanodes ($WO_3/BiVO_4/MeO_x$) modified various metal oxides on a $WO_3/BiVO_4$ at an electric charge of 0.9C (900 s at steady photocurrent of 1 mA) in a 0.5 M $KHCO_3$ aqueous electrolyte (35 mL) in an ice bath (below 5 °C) under simulated solar light.

diffraction peaks derived from MeO_x were observed in all $WO_3/BiVO_4/MeO_x$ photoanodes, suggesting that all tried MeO_x modified on $WO_3/BiVO_4$ photoanode possess amorphous-like structure. As shown in Fig. S3; ESI†, little change of the light harvesting efficiency (LHE) was also confirmed in tried all photoanodes, suggesting that these MeO_x introduced on the $WO_3/BiVO_4$ have little effect to light absorption efficiency on $WO_3/BiVO_4$ photoanode. The time courses of voltages applied between photoanode and a counter electrode of Pt mesh at steady photocurrent of 1 mA (Fig. 2) in oxidative H_2O_2 genera-tion reaction were also confirmed (Fig. S4; ESI†). The voltages for applying steady photocurrent of 1 mA slightly increased by introducing MeO_x on the $WO_3/BiVO_4$ photoanode. In particular, $WO_3/BiVO_4/Al_2O_3$ photoanode, coated uniformly, smoothly and flatly at Al_2O_3 compared to other MeO_x, required highest applied voltage. In order to confirm the effect introducing the Al_2O_3 on the photoanode in more detail, the photocurrent property of the $WO_3/BiVO_4/Al_2O_3$ photoanode was investigated in a 0.5 M $KHCO_3$ aqueous solution (Fig. S5; ESI†). The bare $WO_3/BiVO_4$ photoanode exhibited excellent photocurrent property in all applied voltage ranges as with our past reported example,[11,12,28,29] and the photocurrent property slightly decreased by introducing the Al_2O_3 layer. However, it should be noted that the decreasing degree of the photocurrent property was slight, only *ca.* 9% and 5% at +1.23 V and +1.77 V *vs.* RHE, respectively, although the Al_2O_3, having an insulation property, covered the entire area of the $WO_3/BiVO_4$ photoanode. A similar

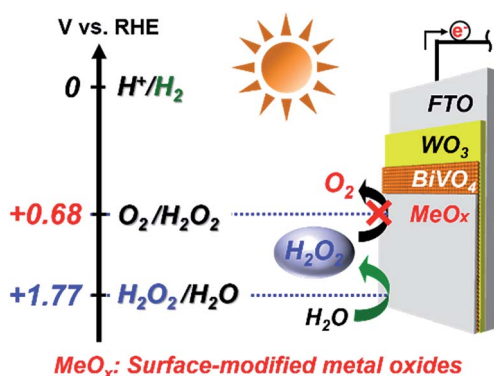Fig. 1 Pattern and energy diagrams for photoelectrochemical H_2O_2 generation from H_2O on $WO_3/BiVO_4/MeO_x$ photoanodes under solar light irradiation.

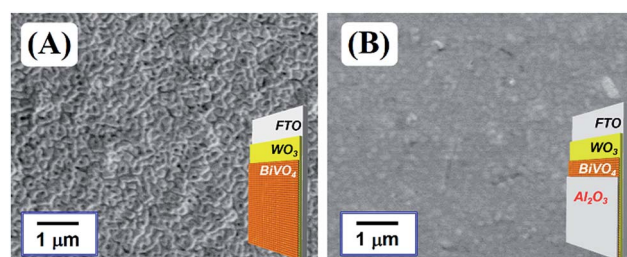Fig. 3 SEM images of (A) $WO_3/BiVO_4$ and (B) $WO_3/BiVO_4/Al_2O_3$ photoanodes.

phenomenon has also been observed in O_2 and H_2 generation through water splitting on a photoanode coated with amorphous-like Ta_2O_5.[32] In addition, it was confirmed, from the N_2 absorption and desorption measurement of MeO_x particles (Fig. S6; ESI†), that almost all MeO_x possess mesoporous structure at a pore size of *ca.* 4–20 nm. In particular, a pore size of the Al_2O_3 was *ca.* 4.7 nm. The thicknesses of Al_2O_3 calculated from the coating amount on the $WO_3/BiVO_4$ photoanode by XRF measurement were *ca.* 100 nm (0.055 mg cm^{-2}). In order to also investigate the effects of dense Al_2O_3 on $WO_3/BiVO_4$ on the oxidative H_2O_2 generation, increasing Al_2O_3 amount on $WO_3/BiVO_4$ photoanode was performed by decreasing the spin coating number (500 rpm) of precursor solution of EMOD solved in butyl acetate containing ethylcellulose when introducing Al_2O_3 layers. The thickness of Al_2O_3 introduced at 500 rpm calculated from the XRF measurement was *ca.* 127 nm (0.070 mg cm^{-2}), suggested that the thickness increases with decreasing the spin coating number. As shown in Fig. S7; ESI,† little change of the H_2O_2 generation amounts was observed on these $WO_3/BiVO_4/Al_2O_3$ photoanodes prepared at 500 and 1000 rpm, indicating that increasing Al_2O_3 on $WO_3/BiVO_4$ photoanode has little effect on the oxidative H_2O_2 generation. In subsequent experiments, $WO_3/BiVO_4/Al_2O_3$ photoanode prepared at 1000 rpm was utilized as the photoanode. These results indicate that the specific effect enhancing oxidative H_2O_2 generation property was achieved on the $WO_3/BiVO_4$ though the mesoporous and amorphous Al_2O_3 layer covered uniformly, smoothly and flatly the entire area.

To track the specific performance enhancing effect of generating H_2O_2 by introducing the Al_2O_3 layer, the concentration dependency of $KHCO_3$ aqueous electrolytes on the oxidative H_2O_2 generation property was investigated at an applied electric charge of 0.9C (Fig. 4(A)). We have already reported that the oxidative H_2O_2 generation property on the $WO_3/BiVO_4$ photoanode was improved with increasing concentration of $KHCO_3$, which acts as an effective catalyst for H_2O_2

generation *via* the two-electron oxidation of H_2O.[28] Even in the case of using the $WO_3/BiVO_4/Al_2O_3$ photoanode, the selectivity ($\eta(H_2O_2)$) for H_2O_2 generation was significantly enhanced with increasing concentration of $KHCO_3$, and the $\eta(H_2O_2)$ in the 2.0 M $KHCO_3$ aqueous solution reached *ca.* 80% at 0.9C, whereas that using the bare $WO_3/BiVO_4$ photoanode was *ca.* 54%. It should be noted that the selectivity ($\eta(H_2O_2) = $ *ca.* 53%) on the $WO_3/BiVO_4/Al_2O_3$ photoanode in lowly concentrated $KHCO_3$ (0.1 M) was comparable to that (*ca.* 54%) on the bare $WO_3/BiVO_4$ photoanode in highly concentrated $KHCO_3$ (2.0 M). This suggests that the Al_2O_3 could effectively be contributing to oxidative H_2O_2 generation from H_2O even in the lowly concentrated $KHCO_3$. Moreover, as shown in Fig. 4(B), the excellent H_2O_2 generation property on the $WO_3/BiVO_4/Al_2O_3$ photoanode compared to the $WO_3/BiVO_4$ photoanode was significantly maintained even at high electric charge up to 50C. As a result, the accumulation amount, using the $WO_3/BiVO_4/Al_2O_3$ photoanode, reached >2500 µM at 50C, while that using the bare $WO_3/BiVO_4$ photoanode was >1300 µM at 50C. The dependency of the applied voltage on the oxidative H_2O_2 generation was investigated to confirm the effect of the Al_2O_3 coating in detail (Fig. S8; ESI†). A small change in H_2O_2 generation performance was observed in all ranges of applied voltages (0.8–1.8 V), suggesting that the enhanced effect of introducing an Al_2O_3 layer is independent of the voltages applied between a photoanode as the working electrode and a Pt mesh as counter electrode using the aqueous electrolyte of the $KHCO_3$.

Although little development with regards to highly selective H_2O_2 generation *via* two-photon oxidation of H_2O and accumulation using photoanodes has been reported, our method of Al_2O_3 coating on the $WO_3/BiVO_4$ photoanode produced tremendous improvement in selective H_2O_2 generation and accumulation from H_2O in a $KHCO_3$ aqueous electrolyte. It is speculated that the specific enhancement of selectivity for H_2O_2 generation on the $WO_3/BiVO_4/Al_2O_3$ photoanode may be caused by a blocking effect, on the mesoporous Al_2O_3 layer, that inhibits oxidative H_2O_2 degradation into O_2 on the $BiVO_4$. To investigate the blocking effect on the Al_2O_3 layer, a degradation property test of H_2O_2 was performed in a 2.0 M $KHCO_3$ aqueous solution containing H_2O_2 (550 µM) in the presence of the bare $WO_3/BiVO_4$ or $WO_3/BiVO_4/Al_2O_3$ photoanodes in presence or absence of simulated solar light irradiation in an ice bath (below 5 °C). In both cases, as shown in Fig. 5, almost all the initial amount of H_2O_2 was maintained in the dark condition, however, the H_2O_2 amount drastically decreased with irradiation by simulated solar light, suggesting that the H_2O_2 was decomposed by photocarriers (excited electrons and holes) produced on the $BiVO_4$. It should be noted that the H_2O_2 degradation in the presence of the $WO_3/BiVO_4/Al_2O_3$ photoanode was dramatically inhibited compared to the degradation in the presence of a bare $WO_3/BiVO_4$ photoanode. The oxidative H_2O_2 generation test was also confirmed in a 2.0 M $KHCO_3$ aqueous electrolyte, initially containing H_2O_2 (210 µM) on the bare $WO_3/BiVO_4$ and $WO_3/BiVO_4/Al_2O_3$ photoanodes, to track the generated H_2O_2 degradation behaviour in more detail (Fig. 6). The generated rates of H_2O_2 were reduced by the initial addition of H_2O_2 in both cases of presence or absence of Al_2O_3.
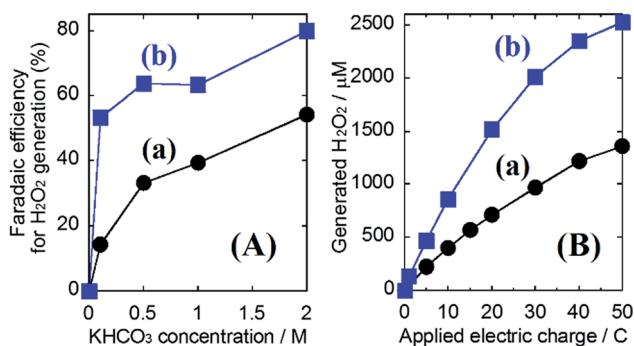

Fig. 4 (A) Oxidative H_2O_2 generation in $KHCO_3$ aqueous electrolytes (35 mL) of different concentrations at applied electric charges of 0.9C (900 s at steady photocurrent of 1 mA) under simulated solar light and (B) accumulation of oxidative H_2O_2 generation in a 2.0 M $KHCO_3$ aqueous solution (35 mL) under visible light irradiation ($\lambda > 420$ nm) using an intense Xe lamp at an applied voltage of 1.5 V in an ice bath (below 5 °C) on a (a) bare $WO_3/BiVO_4$ and (b) $WO_3/BiVO_4/Al_2O_3$ photoanodes.
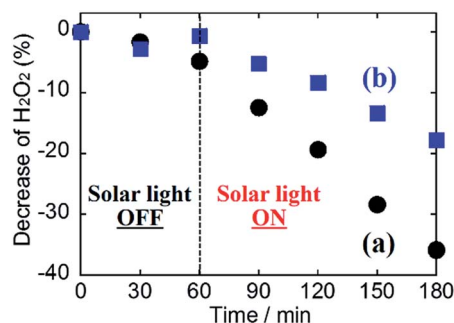
Fig. 5 Degradation properties of H_2O_2 (550 μM) initially added in a 2.0 M $KHCO_3$ aqueous solution in an ice bath (below 5 °C) under CO_2 bubbling and simulated solar light irradiation in the presence of a (a) $WO_3/BiVO_4$ and (b) $WO_3/BiVO_4/Al_2O_3$ photoanodes at no applied voltage.

However, the decreasing rate of H_2O_2 generation was significantly inhibited, from *ca.* 61% to *ca.* 39%, by introducing the Al_2O_3 layer on the $WO_3/BiVO_4$ photoanode. These results suggest that introducing the Al_2O_3 layer significantly contributed to the highly selective H_2O_2 generation and accumulation from H_2O, with a high photocurrent property, by a blocking effect that inhibited the oxidative degradation of generated H_2O_2. The mechanism of blocking effect is proposed that the H_2O_2 generated on the $BiVO_4$ in the $WO_3/BiVO_4/Al_2O_3$ photoanode diffuses in electrolyte of $KHCO_3$ aqueous solution through mesoporous of the Al_2O_3, and contact of the H_2O_2 diffused in electrolyte with the $BiVO_4$ covered uniformly and smoothly Al_2O_3 may be significantly inhibited compared with that with bare $BiVO_4$, resulting in the formation of effective inhibition of oxidative H_2O_2 degradation. Furthermore, there may be other possible mechanisms such as a blocking effect of a direct O_2 evolution site *via* a 4-photon process covering by Al_2O_3, or an enrichment effect resulting from the increasing $KHCO_3$ concentration around the photoanode based on the acid–base adsorption between HCO_3^- (a weak base) and the weakly acidic sites on the Al_2O_3 surface, related to the good

$\eta(H_2O_2)$ in lower $KHCO_3$ concentration, as shown in Fig. 4(A). The tracking and contribution of these other mechanisms, on the Al_2O_3 layer, is currently under investigation.

Conclusions

In summary, various metal oxides were coated onto a $WO_3/BiVO_4$ photoanode to enhance the selectivity (faradaic efficiency) of oxidative H_2O_2 generation, in an aqueous electrolyte of $KHCO_3$, from water under solar light irradiation. Among the various metal oxides, the Al_2O_3 coating, which produced a mesoporous and amorphous structure on the $WO_3/BiVO_4$ photoanode, achieved excellent oxidative H_2O_2 generation at a selectivity of *ca.* 80% and an accumulation of >2500 μM (50C). Interestingly, the Al_2O_3-coated $WO_3/BiVO_4$ photoanode dramatically inhibited oxidative degradation of H_2O_2 generated on the $WO_3/BiVO_4$ photoanode after introducing the Al_2O_3 layer. This study contributes to developing a promising design for a clean H_2O_2 production system that uses only water as the raw material under solar light irradiation. More effective dreamy H_2O_2 generation, at an excellent selectivity close to 100%, can be expected by modifying the surface-treatment technology, and it is currently under investigation.

Conflicts of interest

There are no conflicts to declare.

Acknowledgements

Notes and references

1 A. Fujishima and K. Honda, *Nature*, 1972, **238**, 37.
2 Z. G. Zou, J. H. Ye, K. Sayama and H. Arakawa, *Nature*, 2001, **414**, 625.
3 A. Kudo and Y. Miseki, *Chem. Soc. Rev.*, 2009, **38**, 253.
4 K. Maeda, K. Teramura, D. Lu, T. Takata, N. Saito, Y. Inoue and K. Domen, *Nature*, 2006, **440**, 295.
5 K. Fuku, K. Hashimoto and H. Kominami, *Chem. Commun.*, 2010, **46**, 5118.
6 K. Fuku, T. Kamegawa, K. Mori and H. Yamashita, *Chem.– Asian J.*, 2012, 7, 1366.
7 K. Fuku, R. Hayashi, S. Takakura, T. Kamegawa, K. Mori and H. Yamashita, *Angew. Chem., Int. Ed.*, 2013, **52**, 7446.
8 B. D. Alexander, P. J. Kulesza, I. Rutkowska, R. Solarska and J. Augustynski, *J. Mater. Chem.*, 2008, **18**, 2298.
9 K. Sayama, A. Nomura, Z. Zou, R. Abe, Y. Abe and H. Arakawa, *Chem. Commun.*, 2003, 2908.
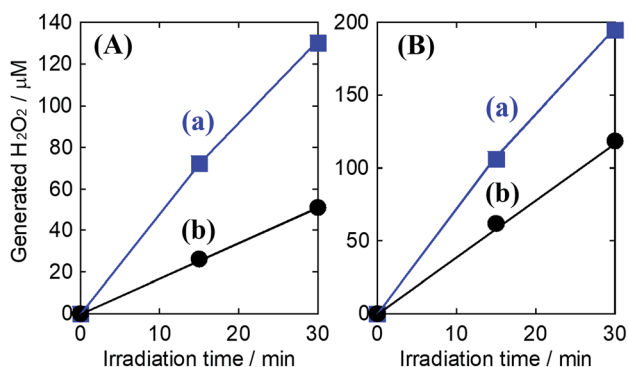10 P. Chatchai, Y. Murakami, S. Kishioka, A. Y. Nosaka and Y. Nosaka, *Electrochim. Acta*, 2009, **54**, 1147.

Fig. 6 Comparison of oxidative H_2O_2 generation in a 2.0 M $KHCO_3$ aqueous electrolyte (a) in the absence of or (b) containing initially-added H_2O_2 (210 μM) in an ice bath (below 5 °C) on a (A) $WO_3/BiVO_4$ and (B) $WO_3/BiVO_4/Al_2O_3$ photoanodes under simulated solar light irradiation at steady photocurrent of 1 mA.

11 R. Saito, Y. Miseki and K. Sayama, *Chem. Commun.*, 2012, **48**, 3833.

12 I. Fujimoto, N. Wang, R. Saito, Y. Miseki, T. Gunji and K. Sayama, *Int. J. Hydrogen Energy*, 2014, **39**, 2454.

13 X. Shi, I. Y. Choi, K. Zhang, J. Kwon, D. Y. Kim, J. K. Lee, S. H. Oh, J. K. Kim and J. H. Park, *Nat. Commun.*, 2014, **5**, 4775.

14 T. W. Kim and K. S. Choi, *Science*, 2014, **343**, 990.

15 Y. Liu, Y. Guo, L. T. Schelhas, M. Li and J. W. Ager III, *J. Phys. Chem. C*, 2016, **120**, 23449.

16 L. H. Hess, J. K. Cooper, A. Loiudice, C. M. Jiang, R. Buonsanti and I. D. Sharp, *Nano Energy*, 2017, **34**, 375.

17 J. Su, L. Guo, N. Bao and C. A. Grimes, *Nano Lett.*, 2011, **11**, 1928.

18 P. M. Rao, L. Cai, C. Liu, I. S. Cho, C. H. Lee, J. M. Weisse, P. Yang and X. Zheng, *Nano Lett.*, 2014, **14**, 1099.

19 I. Grigioni, K. G. Stamplecoskie, D. H. Jara, M. V. Dozzi, A. Oriana, G. Cerullo, P. V. Kamat and E. Selli, *ACS Energy Lett.*, 2017, **2**, 1362.

20 K. Mase, M. Yoneda, Y. Yamada and S. Fukuzumi, *ACS Energy Lett.*, 2016, **1**, 913.

21 F. M. Toma, J. K. Cooper, V. Kunzelmann, M. T. McDowell, J. Yu, D. M. Larson, N. J. Borys, C. Abelyan, J. W. Beeman, K. M. Yu, J. Yang, L. Chen, M. R. Shaner, J. Spurgeon, F. A. Houle, K. A. Persson and I. D. Sharp, *Nat. Commun.*, 2016, **7**, 12012.

22 J. Y. Kim, G. Magesh, D. H. Youn, J. W. Jang, J. Kubota, K. Domen and J. S. Lee, *Sci. Rep.*, 2013, **3**, 2681.

23 Q. Mi, A. Zhanaidarova, B. S. Brunschwig, H. B. Gray and N. S. Lewis, *Energy Environ. Sci.*, 2012, **5**, 5694.

24 J. C. Hill and K. S. Choi, *J. Phys. Chem. C*, 2012, **116**, 7612.

25 K. Ueno and H. Misawa, *NPG Asia Mater.*, 2013, **5**, e61.

26 K. Fuku, N. Wang, Y. Miseki, T. Funaki and K. Sayama, *ChemSusChem*, 2015, **8**, 1593.

27 H. G. Cha and K. S. Choi, *Nat. Chem.*, 2015, **7**, 328.

28 K. Fuku and K. Sayama, *Chem. Commun.*, 2016, **52**, 5406.

29 K. Fuku, Y. Miyase, Y. Miseki, T. Funaki, T. Gunji and K. Sayama, *Chem.–Asian J.*, 2017, **12**, 1111.

30 K. Fuku, Y. Miyase, Y. Miseki, T. Gunji and K. Sayama, *ChemistrySelect*, 2016, **1**, 5721.

31 T. Shiragami, H. Nakamura, J. Matsumoto, M. Yasuda, Y. Suzuri, H. Tachibana and H. Inoue, *J. Photochem. Photobiol., A*, 2015, **313**, 131.

32 R. Saito, Y. Miseki, W. Nini and K. Sayama, *ACS Comb. Sci.*, 2015, **17**, 592.